Crystallization and Compatibility of Poly(vinyl alcohol)/ Poly(3-hydroxybutyrate) Blends: Influence of Blend Composition and Tacticity of Poly(vinyl alcohol)

NAOKO YOSHIE,* YOICHIRO AZUMA, MINORU SAKURAI, and YOSHIO INOUE

Department of Biomolecular Engineering, Tokyo Institute of Technology, Nagatsuta, Midori-ku, Yokohama 226, Japan

SYNOPSIS

Compatibility of a crystalline/crystalline polymer blend, poly(vinyl alcohol) (PVA)/poly(3-hydroxybutyrate) (PHB), was studied by high-resolution solid-state ^{13}C-NMR spectroscopy. The ^{1}H T_1 measurement demonstrated that both the compatibility and the domain size depend on the composition of the blend. The PVA/PHB blend is compatible only when the blend contains a large amount of PVA. The domain sizes of the compatible blend are less than 200 Å. In the pulse saturation transfer (PST) MAS NMR spectra, the carbonyl carbon resonance from PHB showed a downfield shift, which indicates that the compatibility of the PVA/PHB blends is due to the hydrogen-bonding interaction in the amorphous phase. The DSC measurement showed that the compatible blends adopt low crystallinity for both PHB and PVA. The crystallization in these blends is likely to be disturbed by the hydrogen-bonding interaction in the amorphous phase. The compatibility of PVA/PHB is also affected by the tacticity of PVA. The compatible composition range of the syndiotactic-rich PVA/PHB blend is wider than that of the atactic-PVA/PHB blend. It is likely that the capacity to form the hydrogen bond depends on the tacticity of PVA. © 1995 John Wiley & Sons, Inc.

INTRODUCTION

A bacterially synthesized polyester, poly(3-hydroxybutyrate) (PHB), is thermoplastic with a high degree of crystallinity. General characteristics of this polyester are comparable to those of isotactic polypropylene.[1] Bacterial P(3HB) has the advantage of optical activity, biodegradability, and biocompatibility.[1-3] Thus, this polyester has much potential in applications such as surgical sutures, long-term carriers for drugs, and molded plastics. Stiffness and brittleness, however, disturb its utilization as a plastic material.

To obtain PHB-related materials with high mechanical performance, research on finding polymers suitable to be mixed with PHB is being widely carried out. PHB is miscible with poly(ethylene oxide) (PEO),[4,5] poly(vinyl acetate) (PVAc),[6] poly(vinylidene fluoride) (PVDF),[7] and poly(epichlorohydrin) (PECH).[8] PEO is biodegradable, but PVAc, PVDF, and PECH are not biodegradable. Thus, PHB/PVAc, PHB/PVDF, and PHB/PECH should show only partial biodegradability.

We focus on the biodegradable polymers as a partner of the PHB blend. In a previous article,[9] we reported the compatibility of atactic-PVA/PHB blends. Atactic PVA and PHB are both biodegradable crystallizable polymers. We observed the coexistence of the compatible amorphous phase with the crystalline phases of individual component polymers. The aim of this study was to make clear more detailed characteristics of the PVA/PHB blend. We discuss the attracting interaction between PVA and PHB and the composition dependence of this interaction. The domain size of the compatible PVA/PHB blend will be also discussed. The principal tool of our investigation is high-resolution solid-state NMR methods, which are powerful for

* To whom correspondence should be addressed.

Journal of Applied Polymer Science, Vol. 56, 17–24 (1995)
 CCC 0021-8995/95/010017-08

the analysis of the structure and the interactions between component polymers.

Blends of PHB with syndiotactic-rich PVA are also investigated. It has been known that the stereoregularity of a component polymer influences the compatibility of the polymer blend.[10-13]

EXPERIMENTAL

Samples

PHB (M_w 360,000) was purchased from Wako Pure Chemical Industries, Ltd. Atactic PVA (a-PVA, degree of polymerization 2000, degree of saponification 99%) was purchased from Nacalai Tesque. Syndiotactic-rich PVA (s-PVA, degree of polymerization 1690, degree of saponification 99.9%) was kindly supplied by Kuraray Co., Ltd. Tactisities of PVAs were determined by 67.9 MHz ^{13}C-NMR spectroscopy.[14] The triad tactisities are listed in Table I.

PVA/PHB blends were prepared by casting from hexafluoroisopropanol (HFIP), which was kindly donated by Central Glass Co., Ltd. The films were completely dried under vacuum at 60°C to constant weight.

DSC Experiments

DSC thermal data were recorded on a Seiko DSC-20 equipped with an SSC-570 thermal controller. The films were heated from room temperature to 300°C at a heating rate of 10°C min^{-1}. The melting temperatures shown in this article are taken as the peak position.

NMR Experiments

High-resolution solid-state ^{13}C-NMR spectra were obtained at 67.9 MHz on a JEOL GSX-270 spectrometer equipped with a cross-polarization/magic angle spinning (CPMAS) accessory. ^{13}C-CP MAS NMR spectra were measured with a 2 ms contact time, a 10–30 s pulse repetition, a 27 kHz spectral width, 8K data points, and 400–1000 accumulations. All spectra were acquired with high-power dipolar-decoupling (DD) of ca. 60 kHz and MAS at 4.8–5.5 kHz. ^{13}C chemical shifts were calibrated indirectly by the methyl resonance of solid hexamethylbenzene (17.6 ppm relative to tetramethylsilane).

For the observation of the structures in the amorphous phase, pulse saturation transfer (PST) MAS NMR spectra[15] were measured. In an NMR experiment, pulse saturation of ^{1}H spins induces nuclear Overhouser enhancement in ^{13}C resonances. This enhancement is more effective in a relatively mobile phase. Thus, the PST MAS NMR measurement emphasizes ^{13}C resonances in the amorphous phase relative to those in the crystalline phase. PST MAS NMR spectra were measured with a 10–30 s pulse repetition time and 1600–2000 accumulations. To obtain accurate shifts, ^{13}C chemical shifts were calibrated by the methyl resonance of internal solid hexamethylbenzene.

^{1}H spin-lattice relaxation times were determined by a ^{1}H $(180°)_x$-τ-$(90°)_x$ pulse sequence followed by cross polarization to ^{13}C magnetization.[16] Overlapping peaks were resolved by using the LAB ONE NMR 1 program (New Methods Research, Inc.) for spectral analysis.

Table I Triad Tacticity of PVA

	Triad[a]/%			
	mm	mr	rr	T_m/°C
a-PVA	22	50	28	224.0
s-PVA	15	50	35	246.1

[a] mm, mr, and rr indicate isotactic, heterotactic, and syndiotactic triads, respectively.

RESULTS

Thermal Analysis

Figure 1 shows DSC thermograms of 50/50 (wt/wt) PVA/PHB blends. Every blend is characterized by three distinct endothermic peaks, representing the fusion of PHB crystals, the fusion of PVA crystals, and the decomposition of PHB chains in order of increasing temperature. The difference of the melting temperatures of the PVA crystals in the two blends reflects the character of pure PVAs. The melting temperature of pure s-PVA is about 20°C higher than that of a-PVA (see Table I and Figs. 2 and 3). Glass transition temperatures were not observed because of the high crystallinity of the component polymers.

The variations in melting temperature (T_m) and heat of fusion (J per g of component, PHB or PVA) (ΔH_f) with blend composition are shown in Figures 2 and 3. Two blend systems, a-PVA/PHB and s-PVA/PHB, show similar variations in T_m and ΔH_f. The T_m of the PHB phase slightly decreases with increase of the PVA content in both of the a-PVA/PHB and s-PVA/PHB blends, while the T_m of the

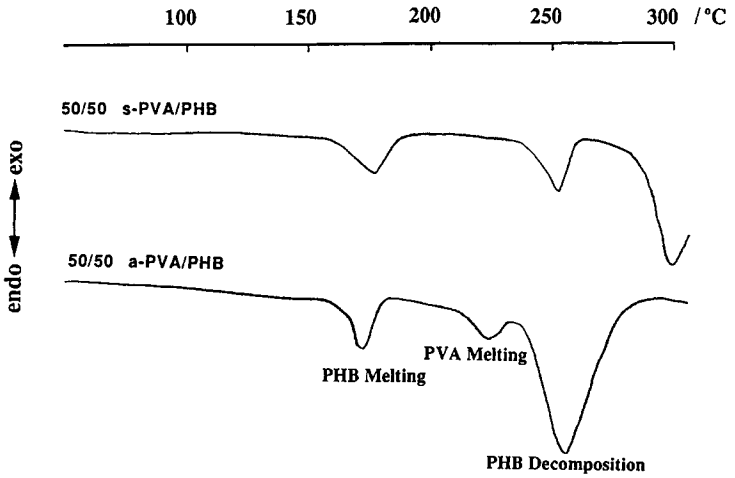

Figure 1 DSC thermograms of 50/50 a-PVA/PHB and 50/50 s-PVA/PHB blends.

PVA phase remains constant. It is likely that PHB and PVA crystallize separately. The morphology of PVA crystals in the blends is considered to be the same as those before blending, while the lamellar of PHB become thinner in the blends than in the pure PHB. The peak representing the fusion of PHB crystals was not observed for the blends containing more than 70 wt % PVA.

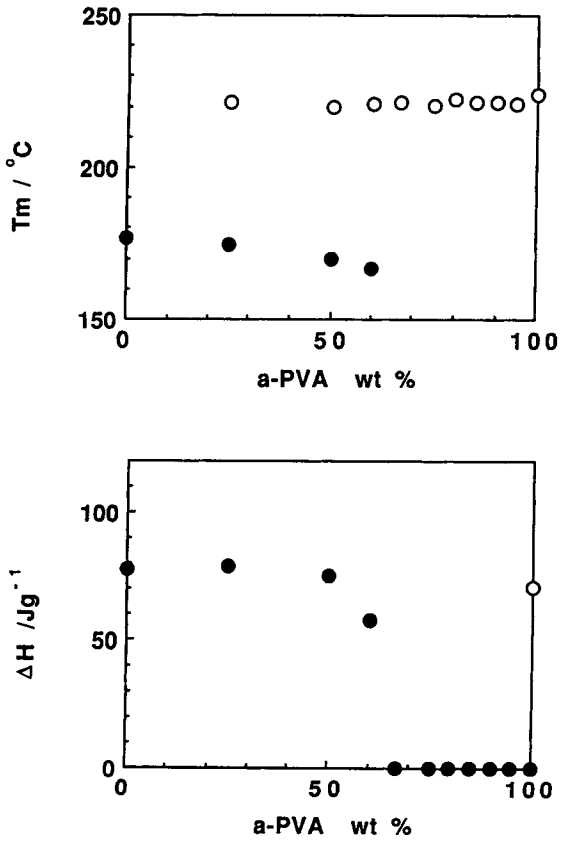

Figure 2 Composition dependence of melting temperature and heat of fusion of (○) a-PVA and (●) PHB in a-PVA/PHB blends.

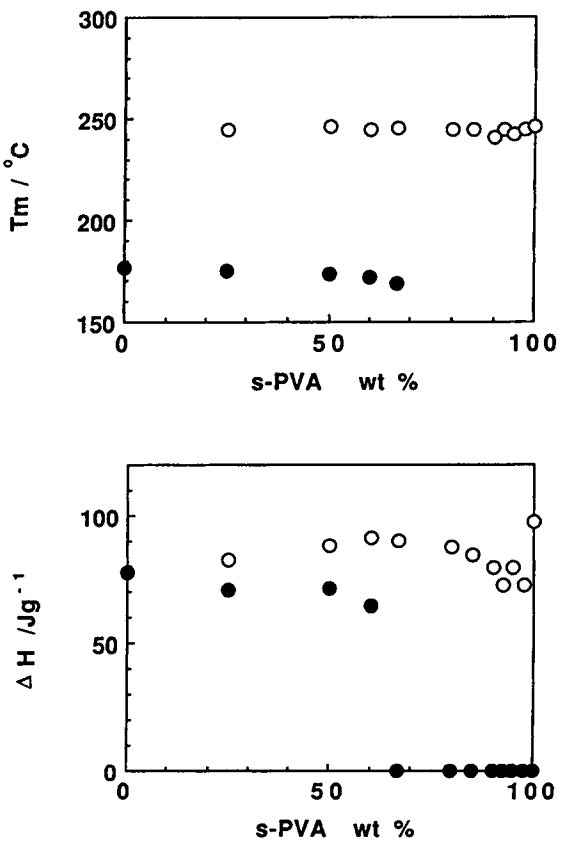

Figure 3 Composition dependence of melting temperature and heat of fusion of (○) s-PVA and (●) PHB in s-PVA/PHB blends.

The ΔH_f of the PHB phase decreases with the increase of the PVA content in both of the blends. Extrapolation of ΔH_f vs. the composition curve indicates that ΔH_f of the PHB phase becomes 0 for the blends containing more than 75 wt % PVA. Thus, no PHB crystals were formed in the blends containing more than 75 wt % a-PVA or s-PVA. The ΔH_f of the s-PVA phase show about a 15% decrease with the decrease of the s-PVA content from 100 to 25 wt %. It is noteworthy that the blends containing 80–97.5 wt % s-PVA exhibit a peculiar small ΔH_f value of the s-PVA phase. In these blends, the crystallinity of s-PVA and PHB should be reduced due to some specific interactions between s-PVA and PHB. If s-PVA and PHB are phase-separated, there is no interaction between them. Thus, the decrease of the crystallinity indicates partial compatibility of these blends. The ΔH_f value of the a-PVA phase could not be estimated from the DSC thermograms because of the overlapping of the peaks of the fusion of a-PVA crystals and the decomposition of PHB chains. Thus, we cannot tell whether the crystallinity of a-PVA also decreases in the a-PVA/PHB blends containing a large amount of a-PVA. However, the data shown below suggests the existence of a similar interaction between PHB and a-PVA. A specific interaction between PVA and PHB will be discussed in the following sections.

Specific Interaction in the Crystalline Phase

If PVA and PHB form a compatible polymer blend, the driving force of the mixing is considered to be an intermolecular hydrogen-bonding interaction between the carbonyl oxygen of PHB and the hydroxyl hydrogen of PVA. For the investigation of the hydrogen-bonding interaction, high-resolution solid-state ^{13}C-NMR spectroscopy is a powerful tool. In general, ^{13}C nuclei participating in hydrogen bonds exhibit more or less characteristic downfield shifts.[17-19] In the case of PVA/polyvinylpyrrolidone (PVP) blends,[19] the formation of the hydrogen-bonding interaction between the carbonyl oxygen of PVP and the hydroxyl hydrogen of PVA results in the downfield shift of about 2 ppm in the carbonyl carbon resonance.

Figure 4 shows ^{13}C-CP MAS NMR spectra of PVA/PHB blends. CP MAS NMR spectra emphasize the resonances from ^{13}C nuclei in the crystalline phase. Thus, the hydrogen-bonding interaction in the crystalline phase can be discussed based on the ^{13}C chemical shift of the carbonyl carbon observed in the CP MAS NMR spectra. In the CP MAS NMR spectra of the blends, the carbonyl resonance from PHB is positioned at ca. 170 ppm and is well resolved from other resonances.

The chemical shift of the carbonyl carbon resonance is independent of the composition for both a-PVA/PHB and s-PVA/PHB blend systems. Thus, we found no detectable hydrogen-bonding interaction between the carbonyl oxygen of PHB and the hydroxyl hydrogen of PVA in the crystalline phase. In these blends, PHB and PVA are expected to crystallize following the phase separation of these polymers. Each component polymer forms separate lamellae. There are no mixed lamellae containing both PVA and PHB. Little variation of the melting temperatures of component polymers with blend composition also supports this result (see Figs. 2 and 3). Considering that cocrystallization in a single lattice is extremely rare for polymer blends, this result is quite reasonable.

It should be noted that the relative intensity of this resonance, in comparison with the PHB content in the blend, becomes small with increase of the PVA content, which indicates decrease of the crystallinity of the PHB phase. This result is consistent with the observation of the heat of fusion (see Figs. 2 and 3).

Specific Interaction in the Amorphous Phase

The structures in relatively mobile (amorphous) phases were investigated by ^{13}C-PST MAS NMR spectroscopy. Figure 5 shows carbonyl carbon resonances in ^{13}C-PST MAS NMR spectra of PVA/PHB blends. The carbonyl resonance shows a significant downfield shift for the blends. Figure 6 shows the shift variation of this resonance with blend composition. The downfield shift was observed for the composition range between 80 and 95 wt % a-PVA or s-PVA, indicating the formation of the hydrogen bonds between the carbonyl oxygen of PHB and the hydroxyl hydrogen of PVA. This hydrogen-bonding interaction should cause the compatibility between PVA and PHB in the amorphous phase. The downfield shift becomes larger as the PVA content increases. No downfield shift was observed for the blends containing less than 75 wt % PVA. Thus, the hydrogen-bonding interaction should become denser with increase of the PVA content. The compatibility between PVA and PHB improves as the PVA content increases. The behavior of the a-PVA/PHB blend is consistent with the results of the previous work.[9]

A ^{13}C-PST MAS spectrum emphasizes the resonances from the amorphous phase, but contains the contributions from ^{13}C included in the crystalline phase. Although the resonances from the crystalline

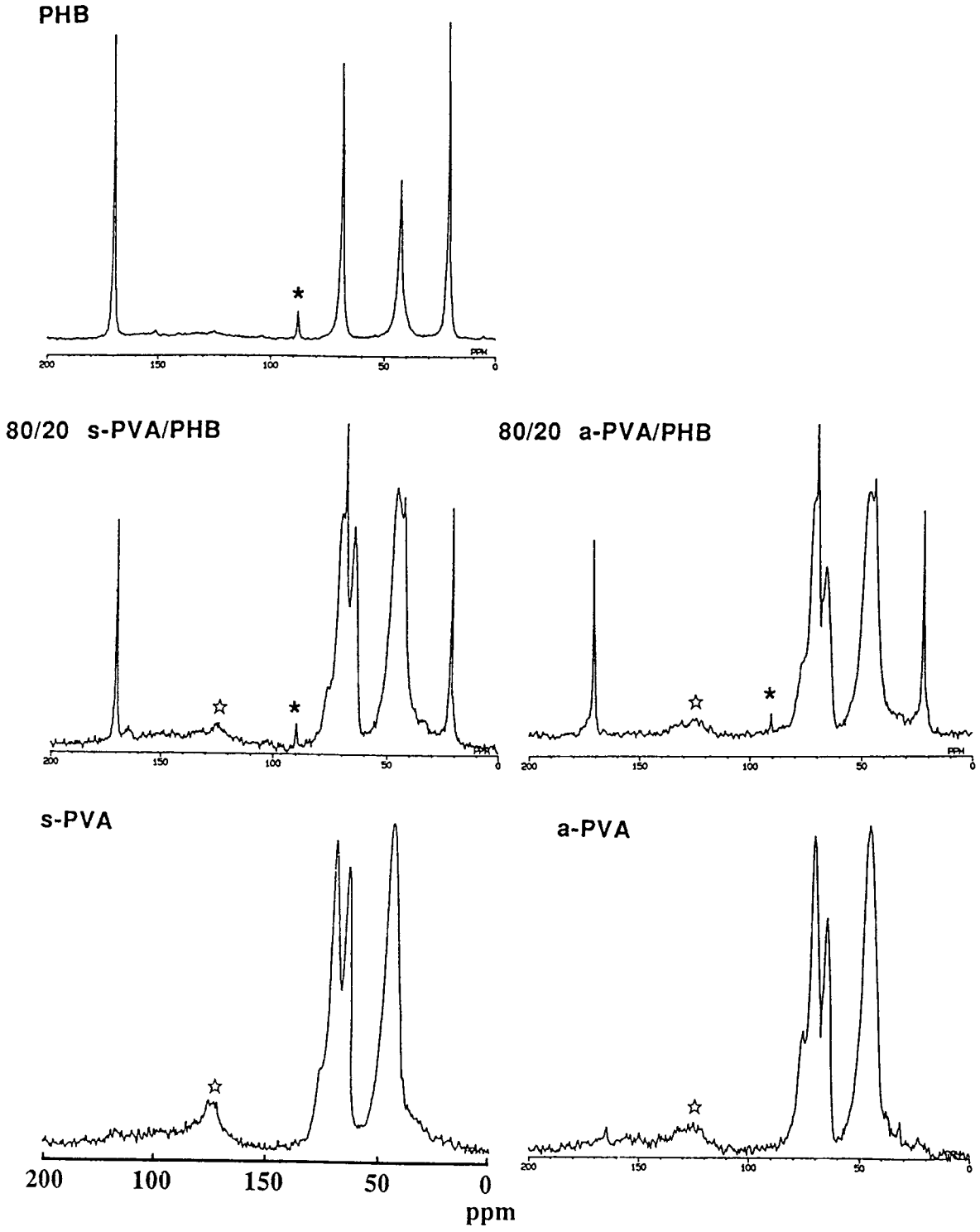

Figure 4 ^{13}C-CP MAS NMR spectra of PHB, a-PVA, s-PVA, and their blends. (*) indicates spinning side band. (☆) indicates the peak ascribed to the sample tube.

phase exhibit small peaks relative to the total number of ^{13}C nuclei in the crystalline phase, the information on the amorphous phase is often screened by the peaks of the crystalline phase for highly crystalline samples. Thus, it is probable that the downfield shift of the amorphous peak is hidden by the

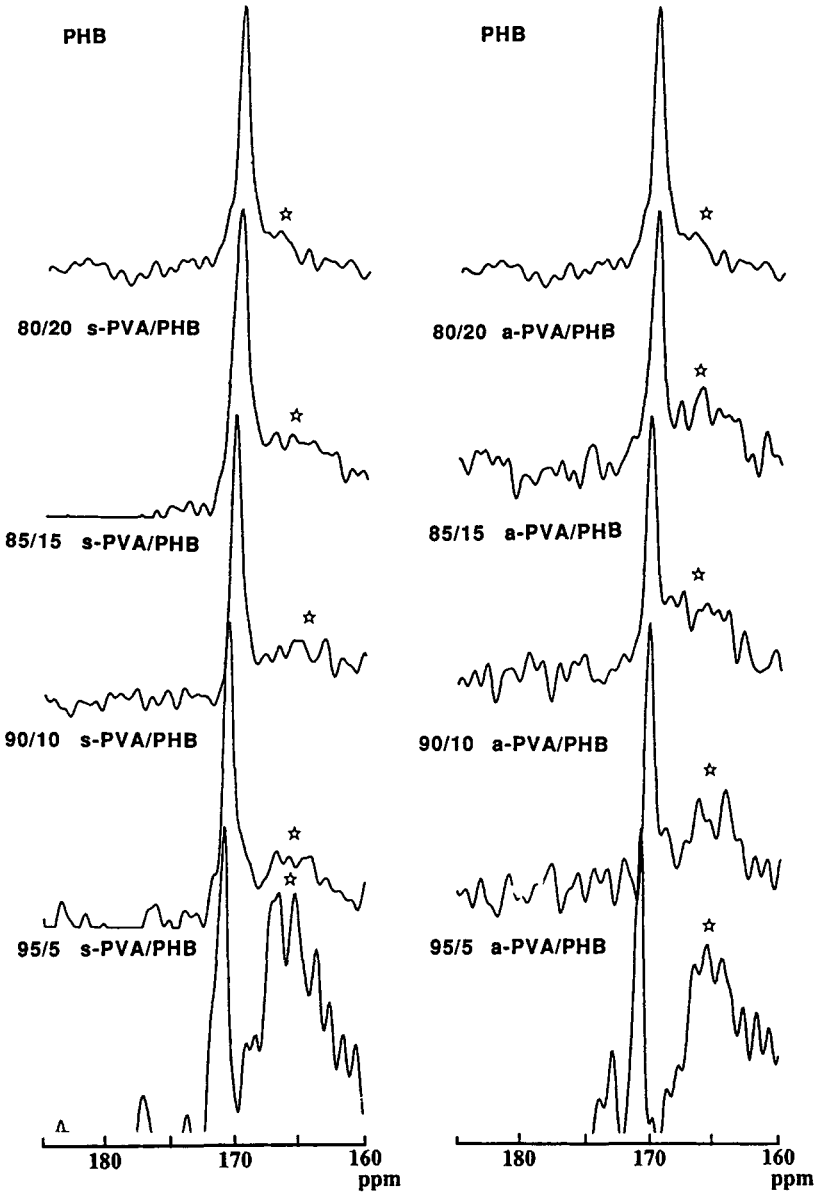

Figure 5 Carbonyl carbon resonances of ^{13}C PST MAS NMR spectra of PHB and blends with a- and s-PVA. (☆) indicates the peak ascribed to the sample tube.

crystalline peak in the blends containing the highly crystalline PHB. The formation of the PHB crystalline phase in the blends containing a large amount of PHB was certainly indicated by the DSC thermograms. Thus, the hydrogen-bonding interaction may also be formed in the blends containing less than 75 wt % PVA.

A slightly more downfield shift was observed for the s-PVA/PHB blend than for the a-PVA/PHB blend. The hydrogen-bonding interaction between s-PVA and PHB is stronger than that between a-PVA and PHB. It is likely that this result reflects that the capacity to make the hydrogen bond differs with the tacticity of PVA. More hydrogen bonds are formed between s-PVA and PHB than between a-PVA and PHB.

Miscibility Between PVA and PHB

The domain size of PVA/PHB blends was studied by observing the ^1H relaxation time T_1 through the CP MAS NMR technique. The ^1H relaxation time study provides information on the domain size. In a polymer blend, each component has inherent ^1H

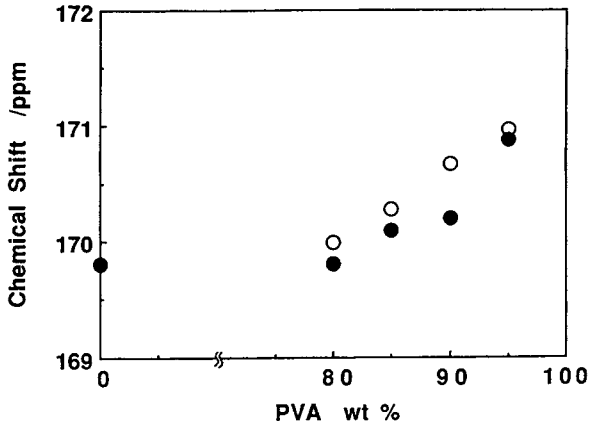

Figure 6 Composition dependence of chemical shift for carbonyl carbon of PHB in ^{13}C-PST MAS NMR spectra of (○) s-PVA/PHB and (●) a-PVA/PHB blends.

relaxation times. If two-component polymers are intimately mixed and the domain sizes of two components are small enough for effective spin diffusion during a ^{1}H relaxation, these components exhibit the same ^{1}H relaxation time. When the domain sizes are larger, each component shows a different relaxation time. A scale for effective spin diffusion during a typical ^{1}H T_1 relaxation is 200–300 Å.

The ^{1}H T_1 values of PHB, PVA, and PVA/PHB blends were measured through methyl and methine carbon resonances. The T_1 value of PHB in the blends was estimated from the decay curve of the methyl carbon. All resonances from PVA in the blends are partially overlapped with the resonances from PHB. Thus, the methine carbon resonances were curve-resolved into two regions ascribed to PVA and PHB, respectively. The decay curve of the resolved resonance provides the T_1 value of PVA in the blends.

Each of the pure polymers, PHB, a-PVA, and s-PVA, shows only one T_1 value. This result indicates that the crystalline and amorphous domains of all the pure polymers are smaller than is the scale of effective spin diffusion. Figure 7 shows the variation of the T_1 value with the blend composition. In the blends, the T_1 values of PHB and PVA approach each other with increasing PVA content. Thus, the compatibility between PVA and PHB improves with increasing PVA content. In the s-PVA/PHB blends containing more than 55 wt % s-PVA, the T_1 values of PHB agree very closely with that of s-PVA, which implies that the domain sizes of s-PVA and PHB are less than 200–300 Å. The s-PVA/PHB blend is compatible in a wider range of composition than is the a-PVA/PHB blend. In the a-PVA/PHB blends containing more than 80 wt % a-PVA, the T_1 values of PHB approach closely that of a-PVA. Thus, the compatibility of these blends is also on a scale of 200–300 Å. The s-PVA/PHB and a-PVA/PHB blends containing less PVA have two distinct T_1 values, each of which is ascribed to the domain composed of one of the component polymers. The domain sizes of these blends is larger than a scale of 300 Å.

DISCUSSION

The ^{1}H T_1 measurement demonstrated the composition dependence of the compatibility between PVA and PHB. The compatibility improves with increase of the PVA content. The s-PVA/PHB blends containing more than 55 wt % s-PVA and a-PVA/PHB containing more than 85 wt % a-PVA are compatible on a scale of 200–300 Å.

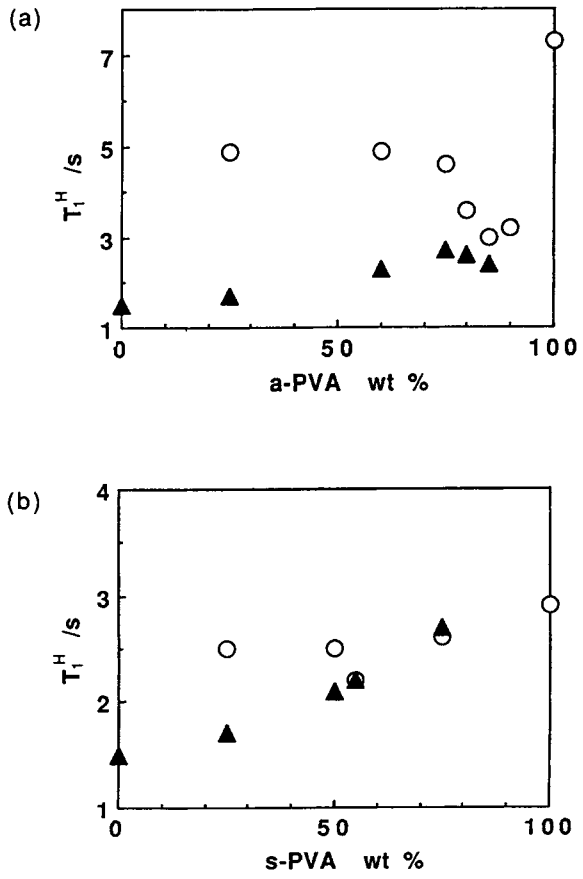

Figure 7 Composition dependence of proton T_1 of (▲) PHB and (○) PVA in (a) a-PVA/PHB and (b) s-PVA/PHB blends.

The downfield shift of the carbonyl carbon resonance in the PST MAS NMR spectra indicates that the compatibility of the PVA/PHB blends is due to the hydrogen-bonding interaction in the amorphous phase. The PVA/PHB blends containing more PVA shows a larger downfield shift, which reflects the denser hydrogen-bonding interaction. The fraction of PHB units participating in the interaction increases with decrease of the PHB content.

The dense hydrogen-bond interaction in the amorphous (melt) phase should prevent the crystallization of PHB, because this interaction disturbs the segregation of the PVA and PHB. The dense hydrogen bonds make the apparent degree of crystallinity smaller. The DSC measurement practically showed the decrease of the crystallinity of the PHB phase in the compatible blends. The decrease of the crystallinity is also observed for the PVA phase in the compatible blends. The compatible blends show low crystallinity for both PHB and PVA phases.

The compatible phase of the PVA/PHB blend should be a quasi-equilibrium phase. Thus, annealing may result in the phase separation and crystallization of the PHB phase. However, the DSC thermogram of 80/20 (wt/wt) PVA/PHB left for 300 days at room temperature is closely similar to that obtained immediately after film preparation. The glass transition temperatures (T_g) of PVA and PHB are ca. 70 and 0°C, respectively. Since the T_g of PVA is much higher than room temperature, the PHB molecules in the compatible amorphous phase are likely to be trapped by the rigid PVA environment.

The compatibility of PVA/PHB is also affected by the tacticity of PVA. The compatible composition range of s-PVA/PHB is wider than that of a-PVA/PHB. It is likely that the capacity to form the hydrogen bond differs with the tacticity of PVA. It is well known that some of the hydroxyl groups in PVA molecules form intramolecular hydrogen bonds between the neighboring monomers in isotactic diad. Thus, the total number of intramolecular hydrogen bonds decreases with the increase of the syndiotacticity of the chain.[20] Only the hydroxyl groups which do not participate in the intramolecular hydrogen-bonding interaction can form the intermolecular hydrogen bonds. Hence, s-PVA has a larger capacity to form the hydrogen bond with PHB than does a-PVA.

This work was partly supported by the Mazda Foundation's Research Grant (1992).

REFERENCES

1. P. P. King, *J. Chem. Tech. Biotechnol.*, **32,** 2 (1982).
2. P. A. Holmes, *Phys. Tech.*, **16,** 32 (1985).
3. E. R. Howells, *Chem. Ind.*, 508 (1982).
4. M. Avella and E. Martuscelli, *Polymer,* **29,** 1731 (1988).
5. M. Avella, E. Martuscelli, and P. Greco, *Polymer,* **32,** 1647 (1991).
6. P. Greco and E. Martuscelli, *Polymer,* **30,** 1475 (1989).
7. H. Marand and M. Collins, *Am. Chem. Soc. Div. Polym. Chem. Polym. Prepr.,* **31,** 551 (1990).
8. E. Dubini Paglia, P. L. Beltrame, M. Canetti, A. Seves, B. Marcandalli, and E. Martuscelli, *Polymer,* **34,** 996 (1993).
9. Y. Azuma, N. Yoshie, M. Sakurai, Y. Inoue, and R. Chûjô, *Polymer,* **33,** 4763 (1992).
10. E. Reordink and G. Challa, *Polymer,* **21,** 509 (1980).
11. C. Marco, J. G. Fatou, M. A. Gomez, H. Tanaka, and A. E. Tonelli, *Macromolecules,* **23,** 2183 (1990).
12. E. J. Vorenkamp, G. ten Brinke, J. G. Meijer, H. Jager, and G. Challa, *Polymer,* **26,** 1725 (1985).
13. G. Beaucage, R. S. Stein, T. Hashimoto, and H. Hasegawa, *Macromolecules,* **24,** 3443 (1991).
14. T. K. Wu and D. W. Ovenall, *Macromolecules,* **6,** 582 (1973).
15. T. Fujito, K. Deguchi, M. Ohuchi, M. Imanari, and M. J. Albright, The 20th Meeting of NMR, Tokyo, 1981, p. 68.
16. M. J. Suilivan and G. Maciel, *Anal. Chem.*, **54,** 1615 (1982).
17. G. E. Maciel and R. V. James, *J. Am. Chem. Soc.*, **86,** 3893 (1964).
18. D. L. VanderHart, W. L. Earl, and A. N. Garroway, *J. Magn. Reson.*, **44,** 361 (1981).
19. X. Zhang, K. Takegoshi, and K. Hikichi, *Polymer,* **33,** 712 (1992).
20. M. Nagura, S. Matsuzawa, K. Yamaura, and H. Ishikawa, *Polymer J.*, **14,** 69 (1982).

Received May 26, 1994
Accepted September 2, 1994